HHS Public Access

Author manuscript

Shock. Author manuscript; available in PMC 2019 November 01.

Published in final edited form as:

Shock. 2018 November ; 50(5): 557–564. doi:10.1097/SHK.0000000000001076.

Sepsis Induces Adipose Tissue Browning in Nonobese Mice But Not in Obese Mice

Itay Ayalon[a], **Hui Shen**[a], **Lauren Williamson**[a], **Keith Stringer**[b], **Basilia Zingarelli**[a], and **Jennifer M Kaplan**[a]

[a]Division of Critical Care Medicine, Department of Pediatrics, Cincinnati Children's Hospital Medical Center, University of Cincinnati College of Medicine, 3333 Burnet Avenue, MLC 2005, Cincinnati, Ohio, USA 45229

[b]Division of Pathology and Laboratory Medicine, Department of Pediatrics, Cincinnati Children's Hospital Medical Center, University of Cincinnati College of Medicine, 3333 Burnet Avenue, MLC 2005, Cincinnati, Ohio, USA 45229

Abstract

Severe sepsis and septic shock are the biggest cause of mortality in critically ill patients. Obesity today is one of the world's greatest health challenges. Little is known about the extent of involvement of the white adipose tissue (WAT) in sepsis and how it is being modified by obesity. We sought to explore the involvement of the WAT in sepsis. We hypothesize that sepsis induces browning of the WAT and that obesity alters the response of WAT to sepsis. Six-week old C57BL/6 mice were randomized to a high fat diet to induce obesity (obese group) or control diet (non-obese group). After 6-11 weeks of feeding, polymicrobial sepsis was induced by cecal ligation and puncture (CLP). Mice were sacrificed at 0, 18 and 72h after CLP and epididymal WAT (eWAT), inguinal WAT (iWAT) and brown adipose tissue (BAT) harvested. Both types of WAT were processed for light microscopy (LM) and transmission electron microscopy (TEM) to assess for morphological changes in both obese and non-obese mice. Tissues were processed for immunohistochemistry (IHC), image analyses and molecular analyses. BAT were used as a positive controls. Non-obese mice have an extensive breakdown of the unilocular lipid droplet and smaller adipocytes in WAT compared to obese mice after sepsis. Neutrophil infiltration increases in eWAT in non-obese mice after sepsis but not in obese mice. Non-obese septic mice have an increase in mitochondrial density compared to obese septic mice. Furthermore, non-obese septic mice have an increase in UCP1 expression. Whereas the WAT of non-obese mice have multiple changes characteristic of browning during sepsis, these changes are markedly blunted in obesity.

Keywords

Sepsis; Obesity; White Adipose Tissue; Lipolysis; Browning

Corresponding Author: Jennifer Kaplan, M.D., M.S., Cincinnati Children's Hospital Medical Center, 3333 Burnet Avenue, MLC 2005, Cincinnati, Ohio 45229, Jennifer.Kaplan@cchmc.org, Phone: 513-636-4259; Fax: 513-636-4267.

Introduction

Sepsis is a syndrome of physiologic, pathologic, and biochemical abnormalities induced by infection. The clinical definition of sepsis in adults was revised based on the current understanding of sepsis-induced changes in organ and tissue function (1). Severe sepsis and septic shock are the biggest causes of mortality in critically ill patients (2). A recent Centers for Disease Control and Prevention (CDC) report suggests that as many as 6% of all reported deaths in the United States could be attributed to sepsis (3).

Obesity is a global epidemic and is one of the world's greatest health challenges, contributing to chronic diseases and burdening health services (4). Morbid obesity is independently associated with increased sepsis risk (5). The effects of obesity on mortality remain controversial as overweight and obese patients may have protection from critical illness in certain diseases, termed the "obesity paradox". Recent studies in adults with obesity and critical illness demonstrated lower mortality rates compared to non-obese patients (6, 7) which is in contrast to early data suggesting the opposite (8). In the pediatric population the data is scant but there is some evidence suggesting positive association between increased body mass index and mortality (9, 10).

Sepsis induces multi-system organ dysfunction in many organs, including the heart, lungs and kidney. These organs are extensively studied both in animal models and translational clinical studies. The adipose tissue however remains a neglected tissue. No longer considered as simply a storage organ for lipids, the adipose tissue is a metabolically dynamic organ capable of synthesizing several biologically active compounds that regulate metabolic homeostasis. Since sepsis is a state in which the metabolic homeostasis is heavily deranged, it is only logical to assume that adipose tissue is involved in the process of sepsis, like any other major organ and therefore deserves more attention.

Recent evidence suggests that adipose tissue undergoes a transformation process known as "browning" in which white adipose tissue (WAT) can adopt a brown adipose tissue (BAT) phenotype in response to various stimuli (11). One of the characteristics of browning is the expression of the uncoupling protein (UCP)-1 (12). UCP1 is a small protein located on the inner membrane of the mitochondria, facilitating proton transport, dissipating the proton gradient while allowing mitochondrial membrane potential to be transduced to heat in a non-shivering pathway (thermogenesis) (13). The process of browning was previously described in states characterized by increased adrenergic stimuli like cold exposure (14), chronic exercise (15), and burns (16). Sepsis is another state characterized by increased adrenergic stimuli but little is known about the association between sepsis and browning. We hypothesize that sepsis induces browning of the WAT but obesity alters this adipose tissue response during sepsis.

Materials and Methods

Animals

The investigations conformed to the Guide for the Care and Use of Laboratory Animals (17) and were approved by the Institutional Animal Care and Use Committee at Cincinnati

Children's Hospital Medical Center. Male C57BL/6 mice at six-weeks of age were obtained from Charles River Laboratories International, Inc. (Wilmington, MA). The mice were housed in the animal facility at the Cincinnati Children's Research Foundation. Food and water were provided ad libitum.

Dietary intervention

At the age of six weeks, animals were randomized to a high-fat diet (TestDiet – 58Y1) (60% kcal provided by fat) or a standard control diet (Formulab – 5008) (16% kcal provided by fat) for six or eleven weeks as indicated. Given the small amount of adipose tissue obtained from non-obese mice it was necessary to extend the dietary intervention beyond six weeks for some experiments. Every high fat-feeding group had its own age-matched control group that received the same duration of dietary intervention. Body weights were monitored weekly throughout the diet phase and are demonstrated in Figure 1 by age cohort at the time of cecal ligation and puncture (CLP).

Induction of polymicrobial sepsis by cecal ligation and puncture

After 6-11 weeks of dietary intervention (at 12 or 17 weeks of age), polymicrobial sepsis was induced by cecal ligation and puncture (CLP) as previously described (18–20). Animals were anesthetized with isoflurane. After opening the abdomen, the cecum was exteriorized and ligated by a 6.0 silk ligature at its base without obstructing intestinal continuity. The cecum was punctured twice with a 22-gauge needle and returned to the peritoneal cavity. The abdominal incision was closed with silk running sutures and liquid topical adhesive. After the procedure, animals were fluid resuscitated with sterile saline (1 ml) injected subcutaneously. All animals received a single dose of intra peritoneal antibiotic (Imipenem 25 mg/kg) and a single dose of subcutaneous analgesia (Buprenorphine 0.05 mg/kg). Animals within each dietary cohort were randomized to either the control group (no CLP - 0h) or were sacrificed at 18 or 72h after CLP (n=4-6 animals/group). Plasma, epididymal WAT (eWAT), inguinal WAT (iWAT) and intra-scapular BAT were collected for analysis. BAT were used as a positive controls.

Immunohistochemistry

Harvested samples of eWAT, iWAT and BAT were fixed in formalin and embedded in paraffin. Sections were stained using hematoxylin and eosin (H&E) and automated immunohistochemistry was performed (Ventana Medical Systems, Tucson, AZ) using anti-UCP1 and anti-myeloperoxidase (MPO) antibodies (Abcam, Cambridge, MA). Whole slide digital images were obtained from the resultant slides using an Aperio AT2 digital slide scanner (Leica Microsystems, Buffalo Grove, IL). The high resolution digital images were analyzed using Image Scope™ software (Aperio version 12) using the positive pixel count algorithm as described by Gannon et al. (21). In brief, the algorithm generates three classes of output values (weak positive, positive, and strong positive) based on pixel intensity which represents staining intensity. Only positive and strong positive values were included in the analysis. Three similar-sized areas were randomly selected on each digital slide and the average value of those three areas was used as the final value for comparison.

Adipose lipid droplet size measurement

Whole slide digital images of mice at 17 weeks of age were obtained for each specimen as described above for IHC. Each image was analyzed using ImageJ software (version 1.48) (22). In brief, three areas in each slide were randomly selected. Twenty adjacent adipocytes in each area were selected and measured for the total lipid droplet surface area. The average lipid droplet surface area was calculated for each sample. The frequency of each adipocyte size was counted.

Transmission electron microscopy (TEM)

Fresh eWAT, iWAT and BAT were fixed in 2.5% glutaraldehyde and 1% paraformaldehyde. Samples were post-fixed in 1% osmium tetroxide in 0.15M sodium cacodylate buffer, processed through a graded series of alcohols, infiltrated and embedded in LX-112 resin. After polymerization at 60 degrees for three days, ultrathin sections (120nm) were cut using a Leica EM UC6 ultramicrotome (Leica Microsystems, Buffalo Grove, IL) and counterstained in 2% aqueous uranyl acetate and Reynold's lead citrate. The ultrathin sections were examined with a Hitachi H-7650 TEM equipped with an AMT digital camera using the AMT Capture Engine 2 software.

Mitochondrial density

Digital TEM images in a predefined magnification (×3000) were used to count the number of mitochondria seen adjacent to the nucleus. To compare the number of mitochondria in each sample, mitochondria number was adjusted to the total surface area in which the mitochondria were located, and termed the "mitochondrial density".

Western blot analysis

Mitochondria were extracted and isolated from frozen eWAT and iWAT (~300 mg) using mitochondria extraction and isolation kits following the manufacturer's protocol (Miltenyi Biotec, Auburn, CA). The Invitrogen NuPAGE gel electrophoresis system (Invitrogen) was used for Western blotting. NuPAGE 10% Bis-Tris gels were used with NuPAGE MOPS buffer and Invitrogen Novex Mini-Cell, BioRad PowerPac 300. Membranes imaged using BioRad ChemiDoc XRS+ gel documentation system and analyzed using ImageLab (version 5.1) software (BioRad, Hercules, CA). The following antibodies were used: anti-UCP1 (Sigma-Aldrich, St. Louis, MO), mitochondrial anti-voltage dependent anion-selective channel (VDAC)-1 protein (Santa Cruz Biotechnology, Dallas, TX).

Enzyme-linked immunosorbent assay (ELISA)

Mitochondria were extracted and isolated from frozen eWAT and iWAT in the same manner as described above in mice aged 17 weeks. UCP1 levels were measured using a mitochondrial UCP1 ELISA kit according to the manufacturer's protocol (MyBioSource, San Diego, CA). Light absorbance was measured at 450 nm using a spectrophotometer (Spectramax plus 384, Molecular Devices). The data were normalized to the original tissue weight and expressed as picogram of UCP1 per gram of tissue.

Measurement of nonesterified fatty acids and triglycerides

Plasma samples from mice aged 17 weeks were measured by enzymatic kit for nonesterified fatty acids (Wako Diagnostics, Mountain View, CA) and triglycerides (Caymen Chemicals, Ann Arbor, MI) per the manufacture's protocol.

Statistical analysis

Data were analyzed using SigmaPlot for Windows Version 13 (SysStat Software, San Jose, CA). For data comparison among two or more interventions, statistical analysis was performed using the two-way ANOVA with Holm-Sidak method for parametric data and the Kruskal-Wallis ANOVA with the Dunn post hoc test for nonparametric data. Data are expressed as mean and standard deviation (SD) for parametric data in the text and figures. A value of $P \leq 0.05$ was considered significant.

Results

Sepsis induces WAT remodeling in non-obese mice which is impaired in obese mice

White adipose tissue is a dynamic and modifiable tissue. With the development of obesity, WAT undergoes a process of tissue remodeling in which adipocytes increase in both number (hyperplasia) and size (hypertrophy). We sought to determine the differences in adipocyte size and determine the changes in adipose tissue in obese and non-obese 12-week-old mice during sepsis. We used H&E stained eWAT and iWAT slides to examine morphologic differences between obese and non-obese mice during sepsis (Figure 2). As expected in eWAT prior to sepsis (CLP 0h), non-obese mice have smaller adipocytes compared to obese mice (Figure 2 – e1, e3 vs. e2, e4). At 18 and 72 hours after CLP, adipocytes decrease in size in non-obese mice and there is an increase in cellular infiltration compared to prior to sepsis (Figure 2 – e5, e7, e9, e11). However, in obese mice, adipocyte size does not change during sepsis when compared to prior to sepsis and there is not a profound cellular infiltration (Figure 2 – e6, e8, e10, e12).

Sepsis causes a significant reduction in lipid droplet surface area in non-obese mice but to a lesser extent in obese mice

To quantify adipocyte size, we measured the mean lipid droplet area in eWAT and iWAT from 17-week-old obese and non-obese mice at 0 and 18 hours after CLP. The mean lipid droplet area in eWAT was lower in non-obese mice compared to obese mice at baseline (0h CLP=non-septic) (3,371±1,841 μm^2 vs. 8,606±1,234 μm^2, $p<0.001$) (Figure 3 – A, C). After sepsis, a 53% reduction in droplet size occurred in non-obese mice compared to baseline (1,564±511 μm^2, $p \leq 0.05$). Septic obese mice had only an 18% reduction in droplet size after sepsis and remained significantly higher compared to non-obese septic mice (7,007±647 μm^2, $p \leq 0.05$). Interestingly, in general, non-obese mice showed more homogeneity in lipid droplet size compared to obese mice regardless of sepsis state. Similar droplet size changes were found in iWAT (Figure 3 – B, C).

Neutrophil infiltration to the eWAT is increased during sepsis in non-obese mice but not in obese mice

To immunohistochemically verify that the cellular infiltrate demonstrated in eWAT after CLP (Figure 2 – e3, e7) was composed of neutrophils, we used an antibody against the neutrophil marker, MPO, and then quantified the positive pixel count using image analysis software. Epididymal WAT from non-obese mice showed an increase in MPO positive pixel count after sepsis compared to non-obese mice at baseline (6,820 ± 4,111 vs. 1,569 ± 335 positive pixel count, $p<0.01$) and compared to obese mice after sepsis (2,310 ± 1,233 positive pixel count, $p=0.001$). Surprisingly MPO positivity was low in iWAT and did not increase after sepsis in obese or non-obese mice.

Sepsis induces a breakdown of the unilocular lipid droplet in non-obese mice but not in obese mice

To further investigate the alterations in WAT morphology during sepsis we examined tissue using TEM in mice aged 12 weeks. In non-obese mice, we found an extensive breakdown of the characteristic unilocular lipid droplet into many different sized lipid droplets (lipid breakdown). Smaller lipid droplets formed from a larger droplet in a process resembling “budding” in which the smaller lipid appeared to be pinched off from the larger droplet (Figure 4 – A, B). Budding was evident at 18 hours after CLP but was more extensive at 72 hours after CLP (Figure 5 – e9, e11, i9, and i11). Budding was abundant in non-obese mice but could only be seen sporadically and to a lesser degree in obese mice (Figure 5). In many instances these newly formed lipid droplets are near mitochondria with direct physical contact between the outer layers of the lipid droplet and mitochondria (Figure 4 – E).

The morphological changes highly suggest that lipolysis is occurring in these tissues. To determine if fatty acids are released during this process we measured fatty acid levels in mice aged 17 weeks. There was no difference in fatty acid levels between non-obese and obese mice at baseline (1.8 ± 0.54 mmol/L and 1.7 ± 0.5, respectively). However, fatty acid levels decreased in both non-obese and obese mice after sepsis (1 ± 0.2 mmol/L and 0.96 ± 0.2, respectively) but there was no dietary effect. We also found no difference in plasma triglyceride levels between non-obese and obese mice at baseline (80 ± 15 mg/dl and 88 ± 23 respectively). Like fatty acid levels, there was a significant decrease in triglyceride levels after sepsis in non-obese and obese mice compared to baseline (39 ± 10 mg/dl and 56 ± 11, respectively). However, triglyceride levels were significantly lower in non-obese septic mice compared to obese septic mice ($p\leq0.05$).

Mitochondrial density increases during sepsis in non-obese mice but not in obese mice

While scanning WAT for ultrastructural changes using TEM, we noticed an increase in the number of mitochondria in the non-obese septic group (Figure 5 – e7 and e11) compared to prior to sepsis (Figure 5 – e3) and compared to the obese septic group (Figure 5 – e8, e12). To quantify the increase in mitochondrial load, we counted the mitochondria in a predefined magnification and adjusted it to the measured surface area to determine the mitochondrial density. Mitochondrial density was significantly higher at 18 hours after CLP in non-obese mice compared to non-septic mice in both eWAT and iWAT (Figure 6). Mitochondrial

density did not change at 18 hours after CLP in obese mice and was significantly lower compared to non-obese mice (Figure 6).

UCP1 expression increases in non-obese mice after sepsis but not in obese mice

Many of the changes described above (i.e. multiple small lipid droplets, increased extracellular matrix between lipid droplets and numerous mitochondria) are known characteristics of brown adipose tissue and the browning process. To provide further evidence of browning during sepsis we investigated changes in the key marker of browning, UCP1. Since UCP1 is a mitochondrial protein, we extracted and isolated eWAT mitochondria and evaluated the mitochondrial extract for UCP1 expression using Western blot analysis. As demonstrated in Figure 7A, UCP1 expression increased in non-obese mice after sepsis (18h after CLP) but did not increase in obese mice after sepsis. As further evidence of changes in UCP1 expression we measured UCP1 expression in isolated mitochondrial extracts from eWAT and iWAT by ELISA. As demonstrated in Figure 7B, UCP1 expression was higher in eWAT from non-obese septic mice compared to non-obese non-septic mice (369 ± 138 vs. 223 ± 72 pg/gr tissue, $p<0.05$) and compared to septic obese mice (226 ± 114 pg/gr tissue, $p<0.01$). Similar changes were demonstrated in iWAT (Figure 7C).

To confirm the above findings, we utilized IHC to determine UCP1 expression and quantified the positive pixel count using image analysis software (ImageScope). eWAT. UCP1 expression was higher at 18 hours after CLP in non-obese mice after sepsis compared to baseline (CLP 0h) (Figure 8A – e3, e1; 7B). Obese septic mice had no significant change in UCP1 expression compared to baseline and expression remained significantly lower compared to non-obese septic mice (Figure 8A – e4, e2; 8B). Similar findings were demonstrated in iWAT (Figure 8A, C).

Discussion

In this study, we demonstrate that sepsis induces adipose tissue browning in non-obese mice but not in obese mice. We found that sepsis induces a breakdown of the WAT unilocular lipid droplet. This leads to a significant reduction in lipid droplet surface area in non-obese mice and to a lesser extent in obese mice during sepsis. Mitochondrial density and UCP1 expression increase during sepsis in non-obese mice but not in obese mice. These morphological changes in non-obese mice are consistent with WAT browning.

Our data demonstrate that during sepsis lipid droplets decrease in size and the unilocular lipid droplet breaks down into multiple smaller droplets, a process called “budding”. This occurs in non-obese mice more than in obese mice. Langouche et al. demonstrated that critically ill patients had smaller adipocytes compared to healthy controls (23). We found similar changes in our murine model of sepsis in which non-obese mice had ~50% decrease in the lipid droplet size during sepsis. Although obese mice had a statistically significant decrease in adipocyte size, this only represented an 18% reduction in adipocyte size during sepsis. Smaller sized adipocytes may represent newly formed adipocytes or cellular breakdown of larger adipocytes. Our TEM results in non-obese septic mice demonstrating

budding of lipid droplets, provide support that smaller adipocytes represent cellular breakdown and lipolysis.

Lipolysis is one of the main functions of adipose tissue and during this process free fatty acids are released for energy utilization. Lipolysis is a regulated function that is initiated by β-adrenergic stimulation and highly coupled to mitochondrial ATP synthesis (24). β-receptor stimulation results in activation of protein kinase-A, hormone-sensitive lipase (HSL) and adipose triglyceride lipase (ATGL) which leads to conversion of triglycerides to free fatty acids. The morphological changes we find highly suggest that lipolysis is occurring in these tissues however we found no difference in fatty acid levels between septic obese and non-obese mice as both groups had decreased levels compared to baseline. Non-obese septic mice had lower plasma triglyceride levels compared to obese septic mice. It is possible that septic non-obese mice have lower triglyceride levels because of increased utilization in other tissues. Alternatively, obese mice may have impaired utilization during sepsis. The fact that obese mice have a larger volume of WAT can potentially lead to an unintentional underestimation of the extent of lipolysis and browning in the obese groups. To minimize this, we sampled several areas from each specimen and used different methods to confirm our findings. Human data demonstrate that people with obesity have evidence of impaired catecholamine-induced lipolysis (25) but other studies show that there is no relationship between obesity status and fasting fatty acid levels (26). Taken together, given the energy demands during sepsis, adipocyte shrinkage and lipolysis would prove beneficial to utilize and breakdown lipids for fuel. But this process is impaired in obese septic mice. Future studies will be necessary to determine whether the morphologic appearance of lipolysis affects metabolic function of the adipose tissue.

In addition to adipocyte breakdown, the number of mitochondria increases in non-obese mice during sepsis but not in obese mice. The increased mitochondrial number may be a mechanism to increase available energy in WAT. Lipid droplet breakdown and lipolysis may provide available energy to the organism and may explain the close physical proximity seen between lipid droplets and mitochondria. However, the interaction between these two structures needs further exploration.

Recent evidence suggests browning occurs in WAT in patients with burn injury and cancer-associated cachexia (16, 27), but until now has not been described in sepsis. To the best of our knowledge, this is the first study to demonstrate that browning occurs in sepsis. Crowell et al. demonstrated WAT UCP1 expression increased during recovery from sepsis (28). We expand on Crowell's findings and confirm an increase in UCP1 expression using three different modalities (IHC, Western blot and ELISA). The increase in UCP1 expression coincided with changes in adipocyte morphology, findings suggestive of browning.

The mechanisms that lead to browning in sepsis remain unknown. One possible initiator of browning is inflammation. It is unclear whether UCP1 expression and browning are dependent on inflammatory cell infiltration. In the current study, adipose tissue neutrophil infiltration, as evidenced by increased MPO, occurred in eWAT from non-obese septic but not obese septic mice. Previous data from our lab also demonstrate that during sepsis, obese mice have a diminished adipose tissue inflammatory response including lower plasma IL-6

levels in early sepsis (29, 30). IL-6 is important for browning (31). Using a chimeric mouse burn model, Abdullahi et al. demonstrate bone marrow derived IL-6 is the main regulator of browning (31). Taken together, these findings suggest that the lack of inflammatory response in obese septic mice may explain the failure of browning.

Unlike brown adipocytes who express high levels of UCP1 under basal (unstimulated) conditions, WAT-induced browning occurs in response to norepinephrine stimulation (32). BAT is highly vascularized and its activation is regulated by the sympathetic nervous system via β-adrenergic receptors (33). Adrenergic stress increases UCP1 expression in both brown and white adipose tissue (11). We hypothesize that since sepsis causes a catecholamine surge and a massive sympathetic response with stimulation of β-adrenergic receptors, it is this process that may initiate WAT browning during sepsis. A limitation to our study is that we did not provide direct measurements of catecholamines and catecholamine receptors. Hahn et al. used a polymicrobial animal model of sepsis and found elevated levels of catecholamines as early as five hours after CLP and levels remained elevated during the acute phase of sepsis (34). Obesity is accompanied by a decrease in β-adrenergic receptor subtypes (35) which could explain, in part, the lack of browning found in obese adipose tissue after sepsis. Future experiments blocking catecholamine receptors may be beneficial and provide additional information clarifying the exact mechanism by which browning occurs in sepsis but are blunted in obesity.

One of the fundamental questions is what advantage, if any, does the browning process provide to the organism? It is possible that browning is merely a way to regulate temperature through increased expression of UCP1 and heat production. Browning may also provide an advantage in the way energy is produced and utilized, given the increased number of mitochondria near multilocular lipid droplets. It is possible that the impaired ability of obese mice to undergo browning contributes to higher mortality. More studies are warranted to understand these processes.

In conclusion, we demonstrate that sepsis induces changes in WAT that are consistent with browning. We consider these changes to be an appropriate physiologic response in non-obese mice to sepsis to provide available energy. However, these changes do not occur in obese mice. Impairment of browning could be an explanation for the higher mortality found in obese mice during sepsis. Further studies will be necessary to pursue these investigations.

Acknowledgments

Funding: NIH R01 GM126551 (JK), R01 GM067202 (BZ), P30DK078392

References

1. Singer M, Deutschman CS, Seymour CW, Shankar-Hari M, Annane D, Bauer M, Bellomo R, Bernard GR, Chiche JD, Coopersmith CM, Hotchkiss RS, Levy MM, Marshall JC, Martin GS, Opal SM, Rubenfeld GD, van der Poll T, Vincent JL, Angus DC. The Third International Consensus Definitions for Sepsis and Septic Shock (Sepsis-3). JAMA. 2016; 315(8):801–10. [PubMed: 26903338]
2. Vincent JL, Marshall JC, Namendys-Silva SA, Francois B, Martin-Loeches I, Lipman J, Reinhart K, Antonelli M, Pickkers P, Njimi H, Jimenez E, Sakr Y, investigators I. Assessment of the worldwide

burden of critical illness: the intensive care over nations (ICON) audit. Lancet Respir Med. 2014; 2(5):380–6. [PubMed: 24740011]

3. Epstein L, Dantes R, Magill S, Fiore A. Varying Estimates of Sepsis Mortality Using Death Certificates and Administrative Codes–United States, 1999-2014. MMWR Morb Mortal Wkly Rep. 2016; 65(13):342–5. [PubMed: 27054476]
4. Collaborators GBDO. Health Effects of Overweight and Obesity in 195 Countries over 25 Years. N Engl J Med. 2017
5. Wang HE, Griffin R, Judd S, Shapiro NI, Safford MM. Obesity and risk of sepsis: A population-based cohort study. Obesity (Silver Spring). 2013; 21(12):E762–9. [PubMed: 23526732]
6. Prescott HC, Chang VW, O'Brien JM Jr, Langa KM, Iwashyna TJ. Obesity and 1-year outcomes in older Americans with severe sepsis. Crit Care Med. 2014; 42(8):1766–74. [PubMed: 24717466]
7. Sakr Y, Alhussami I, Nanchal R, Wunderink RG, Pellis T, Wittebole X, Martin-Loeches I, Francois B, Leone M, Vincent JL, Intensive Care Over Nations I. Being Overweight Is Associated With Greater Survival in ICU Patients: Results From the Intensive Care Over Nations Audit. Crit Care Med. 2015; 43(12):2623–32. [PubMed: 26427591]
8. Bercault N, Boulain T, Kuteifan K, Wolf M, Runge I, Fleury JC. Obesity-related excess mortality rate in an adult intensive care unit: A risk-adjusted matched cohort study. Crit Care Med. 2004; 32(4):998–1003. [PubMed: 15071392]
9. Ross PA, Newth CJ, Leung D, Wetzel RC, Khemani RG. Obesity and Mortality Risk in Critically Ill Children. Pediatrics. 2016; 137(3):e20152035. [PubMed: 26908670]
10. Prince NJ, Brown KL, Mebrahtu TF, Parslow RC, Peters MJ. Weight-for-age distribution and case-mix adjusted outcomes of 14,307 paediatric intensive care admissions. Intensive Care Med. 2014; 40(8):1132–9. [PubMed: 25034475]
11. Cousin B, Cinti S, Morroni M, Raimbault S, Ricquier D, Penicaud L, Casteilla L. Occurrence of brown adipocytes in rat white adipose tissue: molecular and morphological characterization. J Cell Sci. 1992; 103(Pt 4):931–42. [PubMed: 1362571]
12. Jacobsson A, Stadler U, Glotzer MA, Kozak LP. Mitochondrial uncoupling protein from mouse brown fat. Molecular cloning, genetic mapping, and mRNA expression. J Biol Chem. 1985; 260(30):16250–4. [PubMed: 2999153]
13. Lin CS, Klingenberg M. Isolation of the uncoupling protein from brown adipose tissue mitochondria. FEBS Lett. 1980; 113(2):299–303. [PubMed: 7389900]
14. Rosell M, Kaforou M, Frontini A, Okolo A, Chan YW, Nikolopoulou E, Millership S, Fenech ME, MacIntyre D, Turner JO, Moore JD, Blackburn E, Gullick WJ, Cinti S, Montana G, Parker MG, Christian M. Brown and white adipose tissues: intrinsic differences in gene expression and response to cold exposure in mice. Am J Physiol Endocrinol Metab. 2014; 306(8):E945–64. [PubMed: 24549398]
15. Stanford KI, Middelbeek RJ, Goodyear LJ. Exercise Effects on White Adipose Tissue: Beiging and Metabolic Adaptations. Diabetes. 2015; 64(7):2361–8. [PubMed: 26050668]
16. Sidossis LS, Porter C, Saraf MK, Borsheim E, Radhakrishnan RS, Chao T, Ali A, Chondronikola M, Mlcak R, Finnerty CC, Hawkins HK, Toliver-Kinsky T, Herndon DN. Browning of Subcutaneous White Adipose Tissue in Humans after Severe Adrenergic Stress. Cell Metab. 2015; 22(2):219–27. [PubMed: 26244931]
17. National Research Council. Committee for the Update of the Guide for the C and Use of Laboratory A. 2011
18. Zingarelli B, Piraino G, Hake PW, O'Connor M, Denenberg A, Fan H, Cook JA. Peroxisome proliferator-activated receptor {delta} regulates inflammation via NF-{kappa}B signaling in polymicrobial sepsis. Am J Pathol. 2010; 177(4):1834–47. [PubMed: 20709805]
19. Baker CC, Chaudry IH, Gaines HO, Baue AE. Evaluation of factors affecting mortality rate after sepsis in a murine cecal ligation and puncture model. Surgery. 1983; 94(2):331–5. [PubMed: 6879447]
20. Ayala A, Herdon CD, Lehman DL, DeMaso CM, Ayala CA, Chaudry IH. The induction of accelerated thymic programmed cell death during polymicrobial sepsis: control by corticosteroids but not tumor necrosis factor. Shock. 1995; 3(4):259–67. [PubMed: 7600193]

21. Gannon PO, Poisson AO, Delvoye N, Lapointe R, Mes-Masson AM, Saad F. Characterization of the intra-prostatic immune cell infiltration in androgen-deprived prostate cancer patients. J Immunol Methods. 2009; 348(1–2):9–17. [PubMed: 19552894]
22. Schneider CA, Rasband WS, Eliceiri KW. NIH Image to ImageJ: 25 years of image analysis. Nat Methods. 2012; 9(7):671–5. [PubMed: 22930834]
23. Langouche L, Perre SV, Thiessen S, Gunst J, Hermans G, D'Hoore A, Kola B, Korbonits M, Van den Berghe G. Alterations in adipose tissue during critical illness: An adaptive and protective response? Am J Respir Crit Care Med. 2010; 182(4):507–16. [PubMed: 20442437]
24. Fassina G, Dorigo P, Gaion RM. Equilibrium between metabolic pathways producing energy: a key factor in regulating lipolysis. Pharmacol Res Commun. 1974; 6(1):1–21. [PubMed: 4372642]
25. Bougneres P, Stunff CL, Pecqueur C, Pinglier E, Adnot P, Ricquier D. In vivo resistance of lipolysis to epinephrine. A new feature of childhood onset obesity J Clin Invest. 1997; 99(11): 2568–73. [PubMed: 9169485]
26. Karpe F, Dickmann JR, Frayn KN. Fatty acids, obesity, and insulin resistance: time for a reevaluation. Diabetes. 2011; 60(10):2441–9. [PubMed: 21948998]
27. Petruzzelli M, Schweiger M, Schreiber R, Campos-Olivas R, Tsoli M, Allen J, Swarbrick M, Rose-John S, Rincon M, Robertson G, Zechner R, Wagner EF. A switch from white to brown fat increases energy expenditure in cancer-associated cachexia. Cell Metab. 2014; 20(3):433–47. [PubMed: 25043816]
28. Crowell KT, Soybel DI, Lang CH. Inability to replete white adipose tissue during recovery phase of sepsis is associated with increased autophagy, apoptosis, and proteasome activity. Am J Physiol Regul Integr Comp Physiol. 2017; 312(3):R388–R399. [PubMed: 28100477]
29. Kaplan JM, Nowell M, Lahni P, Shen H, Shanmukhappa SK, Zingarelli B. Obesity enhances sepsis-induced liver inflammation and injury in mice. Obesity (Silver Spring). 2016; 24(7):1480–8. [PubMed: 27172993]
30. Kaplan JM, Nowell M, Lahni P, O'Connor MP, Hake PW, Zingarelli B. Short-term high fat feeding increases organ injury and mortality after polymicrobial sepsis. Obesity (Silver Spring). 2012; 20(10):1995–2002. [PubMed: 22334256]
31. Abdullahi A, Chen P, Stanojcic M, Sadri AR, Coburn N, Jeschke MG. IL-6 Signal From the Bone Marrow is Required for the Browning of White Adipose Tissue Post Burn Injury. Shock. 2017; 47(1):33–39. [PubMed: 27648696]
32. Petrovic N, Walden TB, Shabalina IG, Timmons JA, Cannon B, Nedergaard J. Chronic peroxisome proliferator-activated receptor gamma (PPARgamma) activation of epididymally derived white adipocyte cultures reveals a population of thermogenically competent, UCP1-containing adipocytes molecularly distinct from classic brown adipocytes. J Biol Chem. 2010; 285(10):7153–64. [PubMed: 20028987]
33. Peng XR, Gennemark P, O'Mahony G, Bartesaghi S. Unlock the Thermogenic Potential of Adipose Tissue: Pharmacological Modulation and Implications for Treatment of Diabetes and Obesity. Front Endocrinol (Lausanne). 2015; 6:174. [PubMed: 26635723]
34. Hahn PY, Wang P, Tait SM, Ba ZF, Reich SS, Chaudry IH. Sustained elevation in circulating catecholamine levels during polymicrobial sepsis. Shock. 1995; 4(4):269–73. [PubMed: 8564555]
35. Collins S, Daniel KW, Rohlfs EM. Depressed expression of adipocyte beta-adrenergic receptors is a common feature of congenital and diet-induced obesity in rodents. Int J Obes Relat Metab Disord. 1999; 23(7):669–77. [PubMed: 10454099]

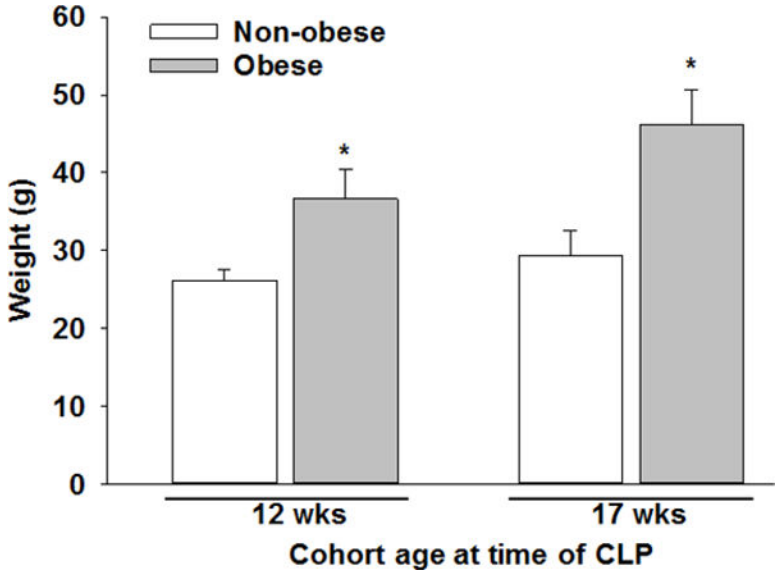

Figure 1. Weight of mice at time of CLP by cohort

At six weeks of age, mice were randomized to a high-fat diet or standard control diet for six (age of 12 weeks at CLP) or eleven weeks (age of 17 weeks at CLP) as indicated. *p≤0.001 vs. non-obese mice as analyzed by t-test.

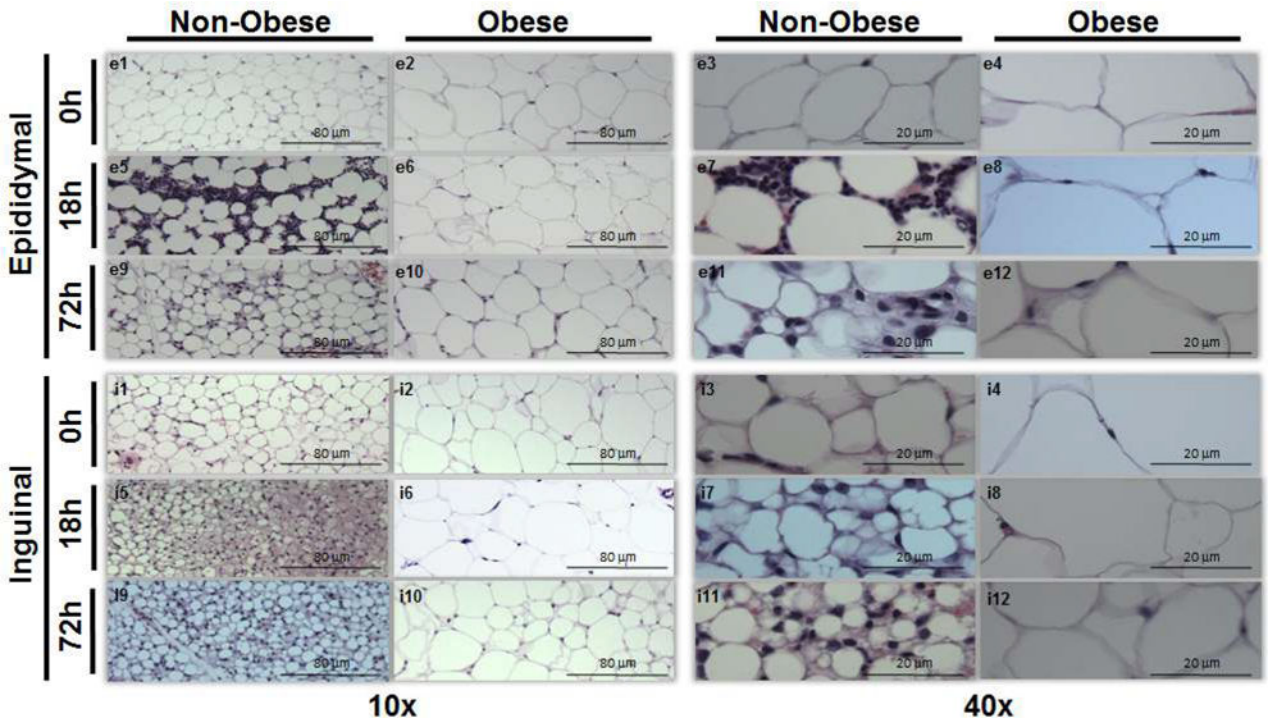

Figure 2. WAT H&E staining from epididymal and inguinal WAT

Epididymal WAT in non-obese mice at 0h (e1,3), 18h (e5,7), and 72h (e9,11) and in obese mice at 0h (e2,4), 18h (e6,8), and 72h (e10,12) after sepsis at 10× and 40× magnification respectively. Inguinal WAT in non-obese mice at 0h (i1,3), 18h (i5,7), and 72h (i9,11) and in obese mice at 0h (i2,4), 18h (i6,8), and 72h (i10,12) after sepsis at 10× and 40× magnification respectively. Representative sections are illustrated. A similar pattern was seen in n=2-4 different samples in each experimental group. All mice were 12 weeks of age at the time of harvest.

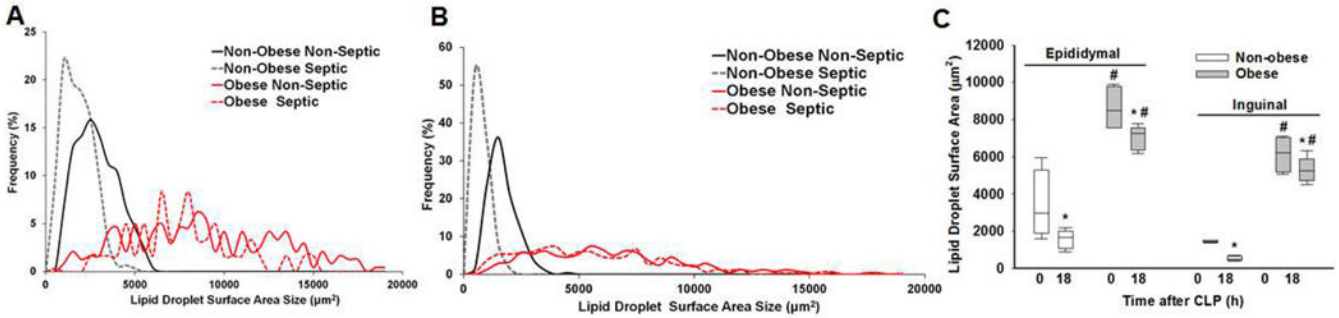

Figure 3. Lipid droplet surface area in non-obese and obese mice at 0 and 18h after CLP by tissue type

Frequency of lipid droplet surface area in (A) eWAT and (B) iWAT from non-obese and obese non-septic and septic (CLP 18h) mice. (C) Lipid droplet surface area in epididymal and inguinal WAT at 0 and 18h after CLP. *p≤0.05 vs time 0h within diet, #p≤0.05 vs non-obese mice by 2-way ANOVA. n= 4-5 mice in each group. All mice were 17 weeks of age at the time of harvest.

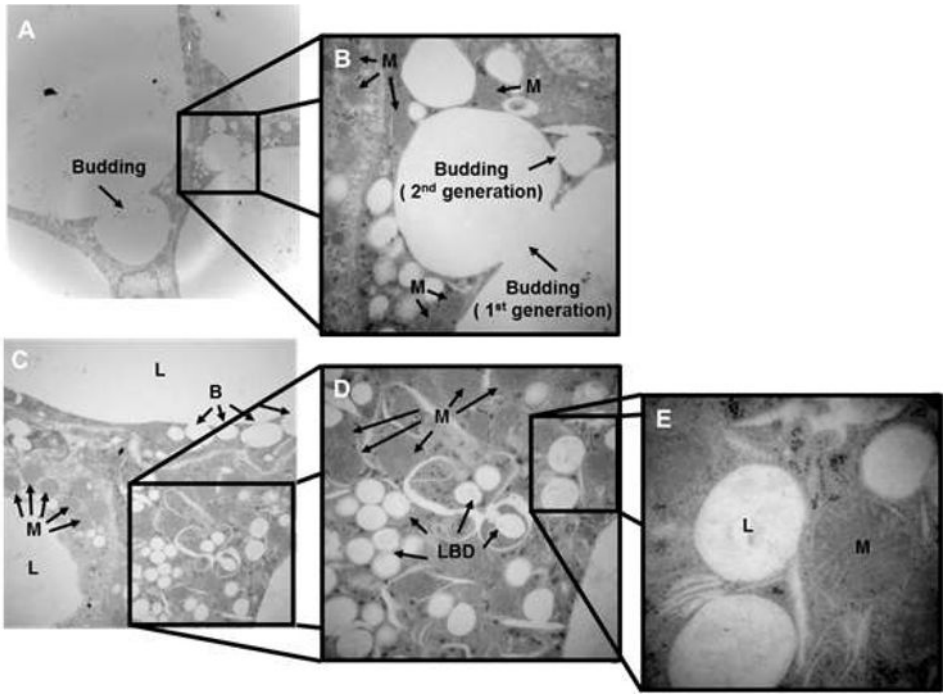

Figure 4. Transmission electron microscopy of epididymal WAT in a non-obese mouse 18 hours after CLP

(A) and (B) demonstrate the budding process in which lipid droplets breakdown into 1st and 2nd generation lipid droplets. (C), (D) and (E) show the close proximity between the newly formed small lipid droplets and mitochondria at 1,500×, 3,000×, 8,000× respectively. Mice were 12 weeks of age at the time of harvest. Representative sections are illustrated. A similar pattern was seen in n=2-4 different samples. L=lipid droplets, B=budding of the lipid droplets, LBD=lipid breakdown, M=mitochondria.

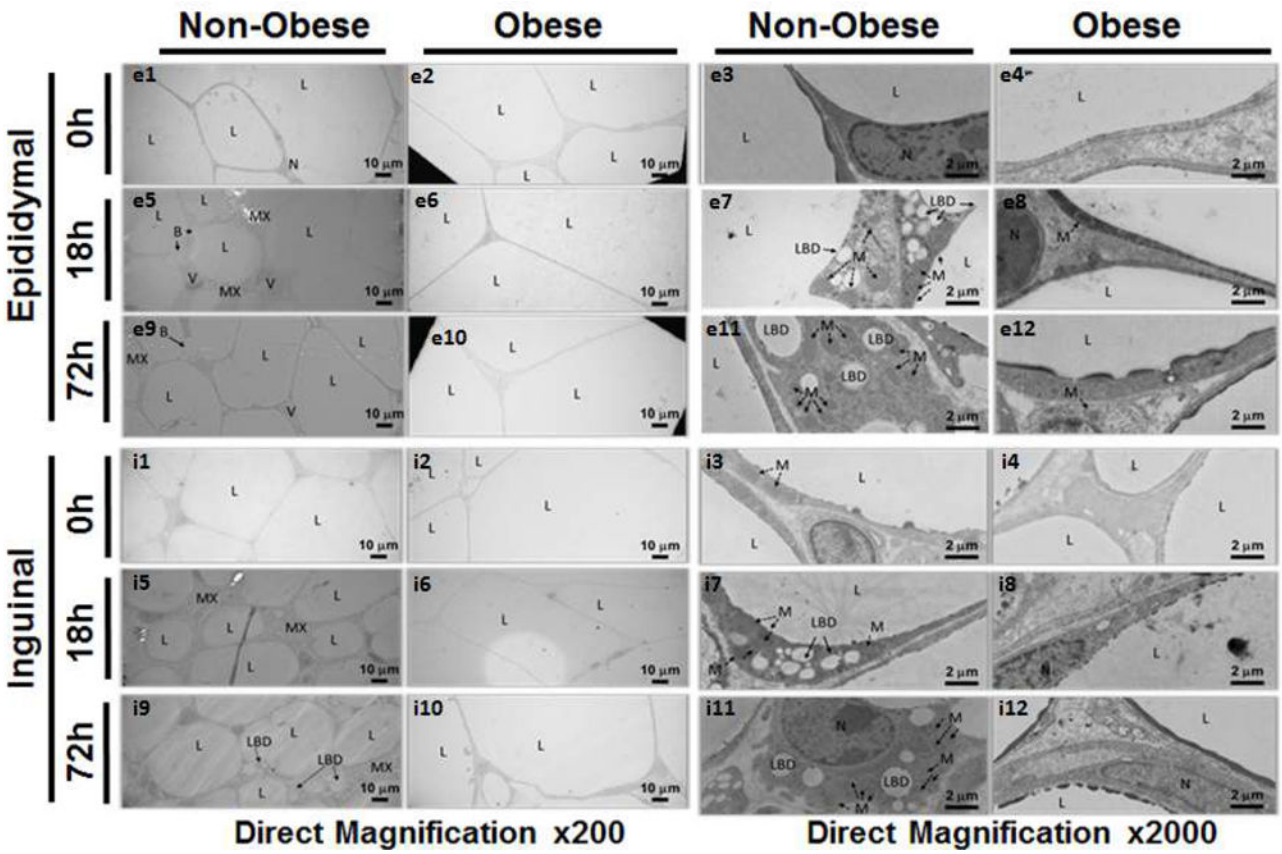

Figure 5. Morphological changes of WAT by Transmission Electron Microscopy in non-obese and obese mice at timepoints after CLP

Epididymal and inguinal WAT in non-obese and obese mice at 0h, 18h, and 72h after sepsis at 200× and 2000× magnification. All mice were 12 weeks of age at the time of harvest. L=lipid droplet, N=nucleus, MX=extracellular matrix, LBD=lipid breakdown, B=budding, M=mitochondria, V=blood vessel.

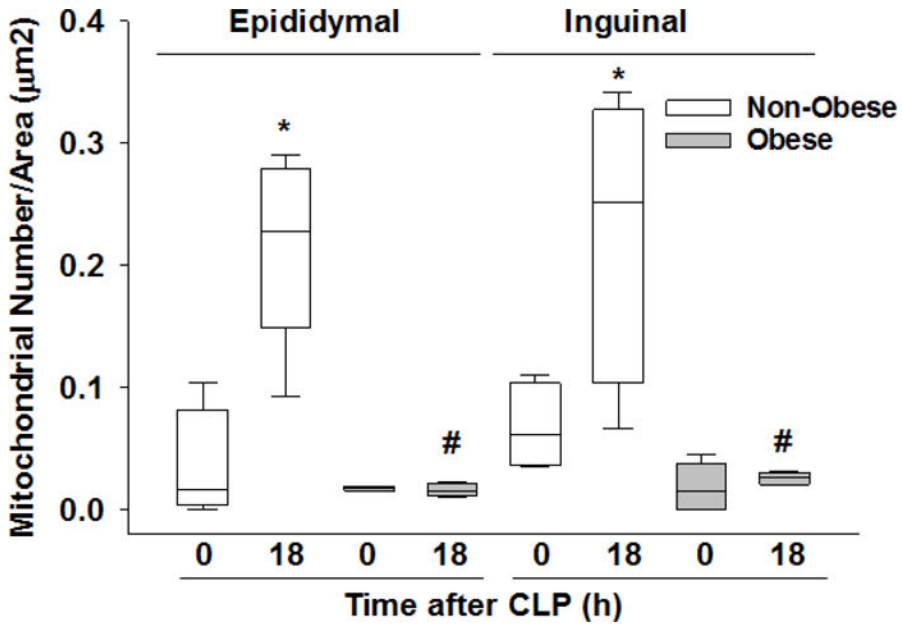

Figure 6. Mitochondrial density in epididymal and inguinal WAT at various timepoints after CLP

Mitochondrial density as calculated by dividing the total number of mitochondria in a predefined magnification (×3000, TEM) by the total measured surface area. All mice were 17 weeks of age at the time of harvest. *p≤0.05 vs time 0h within diet, #p≤0.05 vs non-obese mice by 2-way ANOVA. n= 4-5 mice in each group.

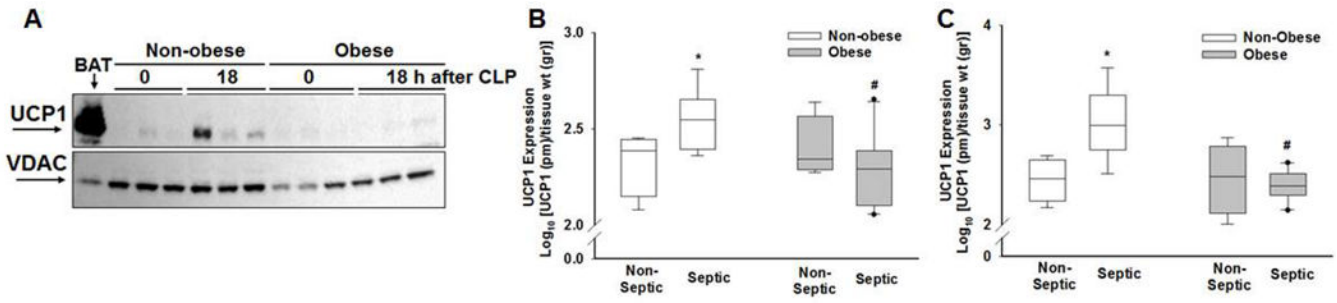

Figure 7. UCP1 protein expression

(A) Mitochondrial UCP1 and VDAC1 (voltage-dependent anion-selective channel-1) expression in iWAT using Western blot analysis. BAT was used as a positive control. Expression of UCP1 in (B) epididymal WAT and (C) inguinal WAT in non-septic (CLP 0h) and septic (CLP 18h) mice. All mice were 17 weeks of age at the time of harvest. *p≤0.05 vs non-septic mice within diet, #p≤0.05 vs non-obese mice by 2-way ANOVA. n= 4-5 mice in each group.

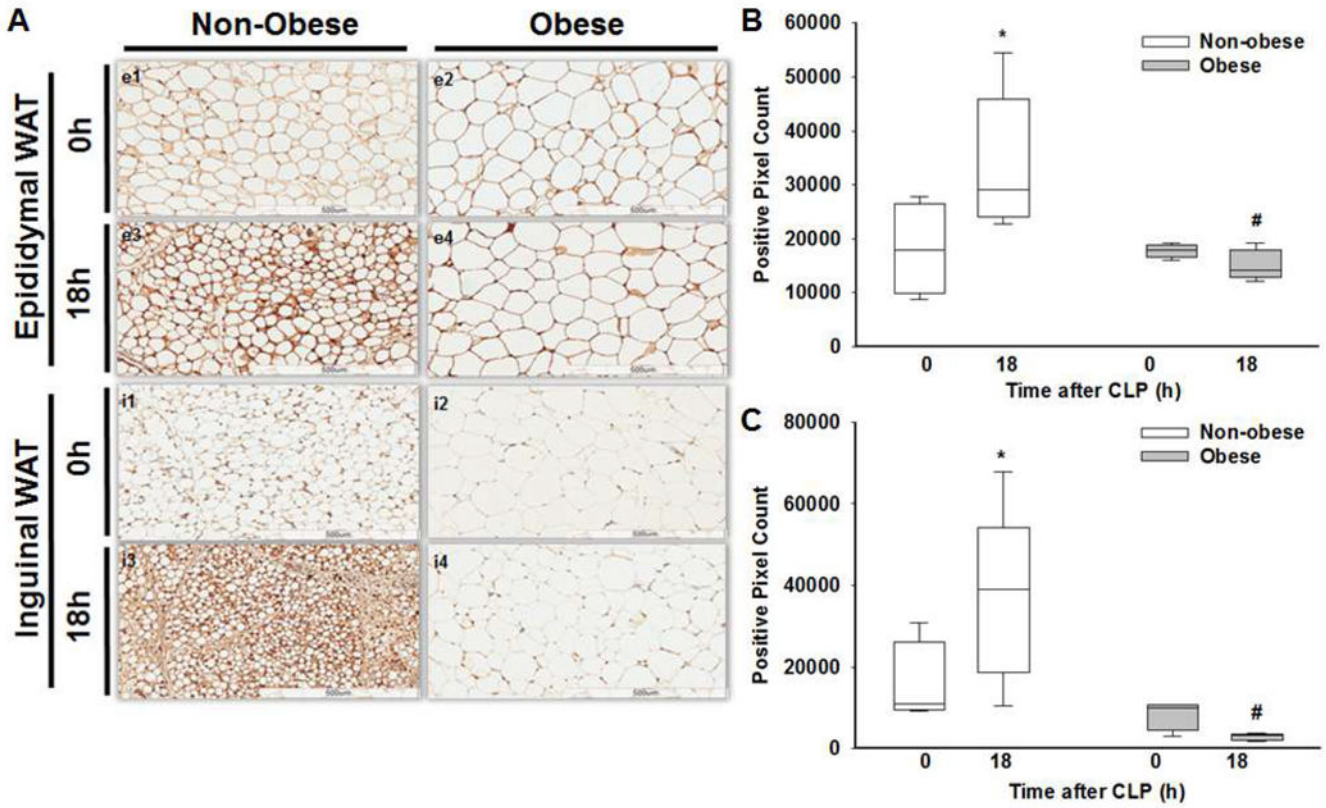

Figure 8. WAT UCP1 expression by immunohistochemistry

(A) Representative images of epididymal WAT UCP1 IHC staining in non-obese mice at 0h (e1), 18h (e3) and in obese mice at 0h (e2), 18h (e4), after sepsis. Inguinal WAT UCP1 IHC staining in non-obese mice at 0h (i1), 18h (i3) and in obese mice at 0h (i2), 18h (i4) after sepsis. Quantification of (B) eWAT and (C) iWAT UCP1 staining using ImageScope software to determine positivity staining of UCP1 intensity in non-obese and obese mice at 0 and 18h after CLP. All mice were 17 weeks of age at the time of harvest. *p≤0.05 vs time 0h within diet, #p≤0.05 vs non-obese mice by 2-way ANOVA. n= 4-5 mice in each group.